European Journal of Human Genetics (2012) 20, 305–312

www.nature.com/ejhg

ARTICLE

Underexpression and abnormal localization of *ATM* products in ataxia telangiectasia patients bearing *ATM* missense mutations

Virginie Jacquemin[1,2,5], Guillaume Rieunier[1,2,5], Sandrine Jacob[1,2,3], Dorine Bellanger[1,2], Catherine Dubois d'Enghien[3], Anthony Laugé[3], Dominique Stoppa-Lyonnet[1,2,3,4] and Marc-Henri Stern*[,1,2,3]

Ataxia telangiectasia (A-T) is a rare autosomal recessive disorder characterized by progressive cerebellar ataxia, oculocutaneous telangiectasia, immune defects and predisposition to malignancies. A-T is caused by biallelic inactivation of the *ATM* gene, in most cases by frameshift or nonsense mutations. More rarely, *ATM* missense mutations with unknown consequences on *ATM* function are found, making definitive diagnosis more challenging. In this study, a series of 15 missense mutations, including 11 not previously reported, were identified in 16 patients with clinical diagnosis of A-T belonging to 14 families and 1 patient with atypical clinical features. *ATM* function was evaluated in patient lymphoblastoid cell lines by measuring *H2AX* and *KAP1* phosphorylation in response to ionizing radiation, confirming the A-T diagnosis for 16 cases. In accordance with previous studies, we showed that missense mutations associated with A-T often lead to *ATM* protein underexpression (15 out of 16 cases). In addition, we demonstrated that most missense mutations lead to an abnormal cytoplasmic localization of *ATM*, correlated with its decreased expression. This new finding highlights *ATM* mislocalization as a new mechanism of *ATM* dysfunction, which may lead to therapeutic strategies for missense mutation associated A-T.
European Journal of Human Genetics (2012) **20,** 305–312; doi:10.1038/ejhg.2011.196; published online 9 November 2011

Keywords: *ATM*; missense mutation; ataxia telangiectasia; pathogenic mutation; subcellular localization

INTRODUCTION

Ataxia telangiectasia (A-T) (MIM#208900) is a rare genetic disorder with autosomal recessive inheritance.[1] A-T features include cerebellar ataxia, oculomotor apraxia, oculocutaneous telangiectasia, immune deficiency, elevated serum α-fetoprotein level and acquired 7 and 14 chromosome translocations in the lymphocyte karyotype. In addition, A-T is characterized by clinical and cellular hypersensitivity to ionizing radiation (IR) and an increased risk of cancer.[2,3] A-T may be difficult to diagnose, particularly in young patients before the appearance of all features of the disease and in milder or atypical cases. Identification of the molecular defect is critical in such cases.

A-T disorder is due to biallelic inactivation of the *ATM* gene (MIM#607585).[4] The *ATM* gene product is a 3056 amino-acid protein that has a central role in the cellular response to DNA damage. This serine/threonine protein kinase belongs to the phosphoinositide 3-kinase-related protein kinase family. *ATM* is mainly activated when DNA double-strand breaks occur, and regulates a complex signaling cascade involved in the detection and repair of this type of DNA damage (for review Lavin[5]). *ATM* is predominantly located in the nucleus, although a fraction of *ATM* has been found associated with peroxisomes.[6] Interestingly, functions independent of DNA damage signaling have been recently reported.[7–9]

A wide variety of mutations have been identified scattered over the entire coding sequence of the *ATM* gene. The majority of these mutations are frameshift or nonsense mutations,[10–13] accounting in our diagnosis series for 73% of cases,[14] suggesting that the classical A-T phenotype is due to total loss of *ATM* protein. *ATM* missense mutations could be responsible for typical,[13] or milder phenotypes,[15,16] but the consequences of many missense mutations not previously associated with A-T remain unknown. Bioinformatics tools are helpful in the latter case but generally insufficient to definitely establish the A-T diagnosis, and direct biological analyses are necessary to determine the pathogenic character of such mutations. Recent studies showed that functional consequences of *ATM* missense variants can be assessed by modeling *ATM* mutations and testing their deleterious effects in complementation assays.[17–19] In both studies, most *ATM* missense mutations in A-T were associated with expression defects and/or kinase activity deficiencies.

In this study, we report the analysis of a series of missense mutations of the *ATM* gene, including 11 not previously reported, identified in 16 patients with clinical diagnosis of A-T belonging to 14 families and 1 patient with atypical clinical features. Deleterious consequences of these mutations were found in all but one case by functional assessments of *ATM* activity, strengthening the A-T diagnosis for 16 patients. We confirmed that *ATM* missense mutations are associated with protein underexpression in all but one A-T patients. Furthermore, we showed for the first time that this underexpression was associated with an abnormal cytoplasmic localization in 12 of the

[1]Institut Curie, Centre de Recherche, Paris, France; [2]INSERM U830, Paris, France; [3]Institut Curie, Hôpital, Service de Génétique, Paris, France; [4]Faculté de médecine Université Paris-Descartes, Paris, France
*Correspondence: Dr MH Stern, INSERM U830, Institut Curie, Centre de Recherche, 26 rue d'Ulm, F-75248 Paris cedex 05, France. Tel: +33 1 56 24 66 46; Fax: +33 1 56 24 66 30; E-mail: marc-henri.stern@curie.fr
[5]These authors contributed equally to this work.
Received 26 January 2011; revised 16 September 2011; accepted 22 September 2011; published online 9 November 2011

16 A-T patients bearing missense mutations. These data suggest a new mechanism accounting for *ATM* deficiency, which may lead to new therapeutic strategies.

MATERIALS AND METHODS

Patient selection and mutation detection

Patients with suspected A-T were referred to the Institut Curie genetic laboratory for *ATM* mutation screening. Blood samples were used for genetic analysis and for lymphoblastoid cell line (LCL) establishment with the informed consent of patients or their parents for young patients. According to Micol *et al*,[14] clinical diagnosis of A-T was made when patients presented ataxia and/or oculomotor apraxia and at least two of the following manifestations: oculocutaneous telangiectasia, recurrent infections, low serum IgA level, high serum α-fetoprotein level (AFP) or karyotype abnormalities such as translocations or inversions of chromosomes 7 and 14. This study include 17 patients harboring *ATM* missense mutations: 16 with clinical diagnosis of A-T and 1 case (38437A1) with non-defined diagnosis, but presenting some features of A-T (ataxia and increased level of AFP).

The 62 coding exons of *ATM* and an average of 30 nucleotides spanning each exon/intron junction were analyzed by direct sequencing of genomic DNA (RefSeq U82828.1). Primer sequences and PCR amplification conditions are available upon request. For compound heterozygote mutations, the presence of one mutation on each parental allele (in trans) was verified when parental DNA was available. The search for large gene rearrangements was performed by semiquantitative PCR, using the Multiplex Ligation-dependent Probe Amplification (MLPA) kit (SALSA MLPA KIT P041/P042 *ATM*, MRC-Holland, Amsterdam, The Netherlands). As nucleotide variations can lead to splicing abnormalities, the genomic sequence environment of each DNA variant was analyzed using Splice Site Prediction by Neural Network (NNSPLICE available at http://www.fruitfly.org/seq_tools/splice.html), MaxEntScan (MES available at http://genes.mit.edu/burgelab/maxent/Xmaxentscan_scoreseq.html).[20] Direct sequencing of the cDNA region surrounding the mutation was performed when a splicing defect was predicted. The *ATM* mutation detection rate in the A-T patients has been estimated to be 96% (292 mutations found in a series of 305 alleles tested).[14]

Patients were selected for this study when at least one *ATM* missense mutation was identified together with available LCL and a clinical diagnosis compatible with A-T.

Cell lines

Epstein–Barr virus-immortalized LCLs were established by Genethon (http://www.genethon.fr/). They were grown in RPMI 1640 (Invitrogen, Oxon, UK) supplemented with 10% fetal calf serum (FCS; Invitrogen), penicillin (0.1 μg/ml) and streptomycin (0.1 μg/ml; Invitrogen) at 37 °C in a humidified incubator with 5% CO_2.

One A-T LCL carrying biallelic *ATM* inactivating mutations (A-T; c.2483delA/p.Lys828SerfsX8 and c.3511C>T/p.Gln1171X) and nine LCLs derived from normal individuals (http://www.genethon.fr/) were used as A-T and wild-type (WT) controls, respectively.

Response to ionizing radiation

Cell lines in exponential growth were seeded at a density of 150 000 cells/ml in 10 ml RPMI 10% FCS in polypropylene round-bottom tubes and irradiated with a dose of 5 Gy using a Cesium γ-irradiator IBL137 (1.73 Gy/min for 175 s) and incubated at 37 °C. Cells were either analyzed for P-*KAP1* (see next paragraph) or fixed at 0 and 1.5 h after irradiation in 70% ethanol for FACS analysis of *H2AX* phosphorylation, according to Olive *et al* with minor modifications.[21] Briefly, cells were resuspended in Tris-buffered saline (TBS), 0.5% Triton, 4% FCS for 10 min at 4 °C and incubated with anti-phosphoSer139-*H2AX* antibody (05-636, 1/1000, Millipore, Billerica, MA, USA) for 1 h at 37 °C. After washing in TBS, cells were incubated with FITC-coupled mouse secondary antibody for 1 h at room temperature (RT). Labeled cells were characterized on a FACS CantoT-MII (BD Biosciences, Franklin Lakes, NJ, USA) and the results were analyzed with Flowjo software (Tree Star, Ashland, OR, USA; v. 8.8.2). Significance of each sample *versus* the WT control was tested by Student's unpaired *t*-test.

Western blot analysis

Cells were collected by centrifugation at 1500 r.p.m. for 10 min at 4 °C and washed in cold phosphate-buffered saline (PBS). Cell pellets were lysed in radioimmunoprecipitation assay buffer (100 mM Tris-HCl/pH7.5, 0.1 M NaCl, 1 mM EDTA, 1% Triton, 0.5% sodium deoxycholate 0.1% sodium dodecyl sulfate (SDS)), supplemented with NaF, Na_3VO_4, phenylmethanesulfonylfluoride (PMSF) and a cocktail of protease inhibitors (Complete, Roche, Basel, Switzerland). A total of 80 μg of protein extracts were separated in a 5% SDS-polyacrylamide gel (SDS-PAGE) and transferred to nitrocellulose membranes. Membranes were blocked in 5% non-fat dry milk for 1 h at RT and incubated overnight at 4 °C with the primary antibodies at the following concentrations: *ATM* (A300-136, 1/2500, Bethyl Laboratories, Montgomery, TX, USA), phospho-Ser824-*KAP1* (A300-767A, 1/1000, Bethyl), β-actin (A-5316, 1/20000, Sigma) and α-adaptin (610502, 1/1000, BD Biosciences) used as a control for protein loading. The secondary antibody coupled to horseradish peroxidase (anti-goat: sc-2020, Santa Cruz Biotechnology, Santa Cruz, CA, USA; anti-mouse: NA931V, and anti-rabbit: NA934V, both from GE Healthcare, Velizy, France) was revealed using the ECL kit (34080, Pierce, Rockford, IL, USA) and band intensities were quantified using ImageJ software (imagej.nih.gov/ij/).

For *ATM* subcellular localization, nuclear and cytoplasmic extracts were prepared using the NE-PER reagents (Pierce) according to the manufacturer's instructions. Corresponding fractions of the cytoplasmic and nuclear extracts from equal cell numbers were separated in 5% SDS-PAGE gel. The purity of each extract was monitored by *MEK1/2* (#9122, 1/1000, Cell Signaling Technology, Danvers, MA, USA) and *INI1* (BAF47-25, 1/1000, BD Biosciences) as specific markers of the cytoplasmic and nuclear compartments, respectively.

Immunofluorescence

Cells were cytospined and fixed for 20 min in PBS 4% paraformaldhyde (PFA), washed in PBS, permeabilized for 10 min in PBS 0.1% SDS. Cells were washed in PBS, blocked for 1 h in PBS 10% bovine serum albumin (BSA), washed in PBS and incubated with anti-*ATM* antibody (NB 100–104, 1/250, Novus Biologicals, Littleton, CO, USA) for 1 h at RT. Cells were washed in PBS, incubated with secondary antibody Alexa Fluor 488 (A21206, 1/50, Invitrogen) for 1 h at RT in the dark. Slides were air-dried and mounted in VectaShield (H1200, Vector Laboratories, Burlingame, CA, USA) with DAPI.

Images were captured using a MicroMax camera (Princeton Instrument, Trenton, NJ, USA) connected to a Zeiss Axioplan 2 fluorescence microscope (Carl Zeiss, Le Pecq, France) with a 100×/1.3 oil immersion objective. Acquisitions were made using the MetaMorph software (Universal Imaging, Burbank, CA, USA). The images were then imported in ImageJ, pseudocolored and merged using the same software.

Quantitative RT-PCR analysis

RNA was extracted using Trizol Reagent (Invitrogen). *ATM* expression with respect to the housekeeping gene *GAPDH* was evaluated by real-time quantitative PCR using the SYBR system according to the manufacturer's protocol (Applied Biosystems, Carlsbad, CA, USA). Amplification of 50 ng of DNase-digested retrotranscripted RNA was performed using the following primers: *ATM*_F 5′-CCTTGGCTACAGATTGCAACC-3′, *ATM*_R 5′-ACTTCCGTAAGG-CATCGTAACAC-3′, *GAPDH*_F 5′-TGCACCACCAACTGCTTAGC-3′ *GAPDH*_R 5′-GGCATGGACTGTGGTCATGAG-3′. Fluorescence intensity was measured by a 7500 Real-Time PCR system (Applied Biosystems) and normalized by the $2^{-\Delta\Delta CT}$ method. Gene expression in three control cell lines was used for baseline expression. Significance of each sample *versus* the WT controls was tested by Student's unpaired *t*-test.

RESULTS

Patients and mutations

A series of 17 patients with clinical features compatible with A-T, belonging to 15 families (2 patients in 2 families) and presenting at least 1 *ATM* missense mutation with unknown consequences on *ATM* function was studied. The clinical and laboratory features of these patients are reported in Table 1. All patients presented ataxia with variable ages at onset from 1 to 10 years old and half presented at least 5 of the 6 A-T criteria. One patient (38437A1) presented only two

Table 1 Clinical and laboratory features of the 17 patients bearing *ATM* missense mutations

Patient	Cerebellar syndrome (age at onset)	Telangiectasia (age at onset)	7–14 Rearrangements (7–14/number of mitoses)	IgA[a]	Recurrent infections	AFP (ng/ml) (normal <10 after 2 y)	Other symptoms
32760A2	Ataxia (2 y)	+	+ (5/67)	5%	+	275 at 9 y	
38633A1	Ataxia (6 y) oculomotor apraxia (9 y)	+	+ (2/50)	10%	No	<10	
9793A1	Ataxia, oculomotor apraxia (8 y)	+	+ (6/30)	8%	No	322 at 43 y	Hypersensibility to radiation, hand dysgenesis, myoclonies, breast cancer at 43 y
38892A2	Ataxia (1 y)	+	+ (5/50)	5%	+	140 at 5 y	
38892A6	Ataxia (1 y)	+	No	24%	No	322 at 8 y	
32753A6	Ataxia (1 y)	+	+ (5/50)	No decrease	No	56 at 9 y	
38437A1	Ataxia (3 y)	Absent at 7 y	No	No decrease	No	39 at 3 y	Cerebral palsy facial dysmorphy
38563A1	Ataxia (2 y)	+	+ (2/25)	No decrease	NA	43 at 3 y	
39039A4	Ataxia (2 y) oculomotor apraxia	Absent at 5 y	+ (2/31)	2.5%	+	37 at 6 y	
39137A1	Ataxia (1 y) oculomotor apraxia	+	+ (5/100)	No decrease	No	40 at 10 y	
40362A1[b]	Ataxia (10 y)	Absent at 31 y	+ (5/100)	ND	No	92 at 29 y	
41832A1	Ataxia (1 y)	+	+ (2/80)	25%	+	687 at 7 y	
53011A1	Ataxia (1 y) oculomotor apraxia	+ (5 y)	+ (1/30)	No decrease	No	42 at 5 y	
56525A2	Ataxia (1 y) no oculomotor apraxia (2 y)	+	No (50)	15%	+	80 at 2 y	
60669A1	Ataxia (1 y)	+ (6 y)	+ (5/100)	No decrease at 6 y	No	26 at 6 y	
63021A1	Ataxia (2 y)	+	+ (2/100)	2%	NA	337 at 15 y	Amyotrophy
63021A2	Ataxia (1 y)	+	ND	7%	+	111 at 10 y	

Abbreviations: AFP, α-fetoprotein; NA, not available; ND, not done; WT, wild type; y, year old.
[a]Expressed as a percentage of age-matched WT controls.
[b]Sister with similar mild A-T.

criteria and additional clinical features such as facial dysmorphia and cerebral palsy, which are not typical in A-T. Karyotypes were available for at least one patient per family in the 15 families and were characteristic of A-T in 13 families (Table 1).

As shown in Table 2, 15 different *ATM* missense mutations were found in these patients, including 11 mutations never previously described in A-T patients (http://chromium.liacs.nl/LOVD2/home.php, http://www.hgmd.cf.ac.uk/ac/index.php). Half of these mutations (7 out of 15 mutations) were located in codons 2401 to 3056, containing the phosphoinositide 3-kinase catalytic domain; a single mutation (p.Arg386Gly in case 53011A1) was within the Nuclear Localization Sequence (NLS, ^{385}KRKK^{388}).[22] Using the A-GVGD algorithm (http://agvgd.iarc.fr/agvgd_input.php),[23] which predicts substitution effects based on assessment of chemical dissimilarity between residues and phylogenetic conservation, 3 missense mutations were considered to be unlikely to be pathogenic (score $\leq$C15), 2 moderately likely to be pathogenic (C25 or C35) and 10 likely to be pathogenic (score $\geq$C45). No consequence of these missense mutations on splice was evidenced. In addition, two single nucleotide polymorphisms (SNP) leading to an amino-acid change were associated with missense mutations in patient 41832A1 (c.378T$>$A;p.Asp126Glu as rs2234997) and in patient 38437A1 (c.3383A$>$G; p.Gln1128Arg as rs56398245).

Direct evaluation of the effects of missense mutations was possible in 14 of the 15 families, as these mutations were either homozygous or associated with a clearly pathogenic allele (nonsense, frameshift or splicing mutations). Separate analysis of each missense mutation was not possible in one cell line carrying two different missense mutations in trans.

ATM function

To confirm the A-T diagnosis in these families, functional approaches assessing the capability of *ATM* to phosphorylate *H2AX* and *KAP1* were performed. FACS analysis of *H2AX* phosphorylation (γ*H2AX*) after IR was shown to correctly discriminate A-T cell lines from cell lines derived from normal individuals as well as from related syndromes such as Nijmegen Breakage Syndrome, A-T-like disease, Friedreich ataxia and ataxia with oculomotor apraxia type 2 (AOA2).[24] LCLs were irradiated at a dose of 5 Gy and the *H2AX* phosphorylation status was measured by FACS at the peak of phosphorylation (1.5 h). As shown in Figures 1a and b, the intensity of the γ*H2AX* peak was markedly decreased in an A-T control cell line as compared with nine WT cell lines. The 16 A-T cell lines with *ATM* missense mutations presented a significantly decreased response to IR similar to that of an A-T control cell line. Interestingly, the cell line derived from case 38437A1 with undefined diagnosis presented normal response to IR.

We next assessed the phosphorylation of another *ATM*-dependent target, *KAP1*, in response to IR.[25] Consistently with the γ*H2AX* assay, we found an impaired response to IR for all *ATM* mutant cell lines but 38437A1 (see Figure 1c and Supplementary Figure 1). Interestingly, two cell lines (40362A1 and 53011A1) presented residual phosphorylation of *KAP1*. Again, the cell line derived from case 38437A1 with undefined diagnosis presented normal response to IR on *KAP1* phosphorylation.

ATM expression

To test the effect of each missense mutation on *ATM* expression, western blot analysis was performed on LCLs established from patients (Figure 2). The antibody used for *ATM* detection specifically recognizes residues 2550–2600, an epitope not directly modified by the mutations in this series of patients. As expected, no *ATM* protein was detected in the control A-T cell line. Level of *ATM* protein expression was markedly decreased in 3 cases ($<$20% expression of the *ATM* level

Table 2 *ATM* status in 17 LCLs bearing *ATM* missense mutations

	Genomic	*Protein*	*Consequences and A-GVGD score*	*ATM transcript % of WT*[a]	*ATM protein % of WT*[a]	*Nuclear ATM % of total*[a]
32760A2	c.7462T>C	p.Cys2488Arg[b]	C65	54±5	17±14	20±18
	c.138_141del4	p.His46_Ser47>GlnfsX9	Frameshift			
38633A1	c.7570G>C	p.Ala2524Pro[b]	C25	55±5	45±12	58±6
	c.3663G>A	p.Trp1221X	Stop			
9793A1	c.5189G>T	p.Arg1730Leu	C0	51±4	11±5	11±6
	c.8585del87	p.2862del29aa	Exon skipping			
38892A2	c.7879T>C (Hmz)	p.Tyr2627His	C65	65±11	24±9	37±18
38892A6	c.7879T>C (Hmz)	p.Tyr2627His	C65	78±12	54±30	40±18
32753A6	c.8124T>A	p.Asp2708Glu	C35	55±8	8±4	40±9
	c.8251_8254del4	p.Thr2751_Ile2752>SerfsX54	Frameshift			
38437A1	c.488A>G	p.Gln163Arg	C0	85±17	87±17	58±10
	c.3383A>G	p.Gln1128Arg[c]	C0			
	c.8419-54del6	NA	Unknown			
38563A1	c.7879T>C (Hmz)	p.Tyr2627His	C65	87±12	42±7	34±6
39039A4	c.8122G>A	p.Asp2708Asn[b]	C15	51±2	23±13	19±17
	c.3712_3716del5	p.Leu1238_Leu1239>LysfsX6	Frameshift			
39137A1	c.6761A>C	p.His2254Pro	C65	57±15	36±15	43±12
	c.3576G>A	p.Ser1135_Lys1192del	Exon skipping			
40362A1	c.6203T>C (Hmz)	p.Leu2068Ser	C55	108±21	59±20	48±10
41832A1	c.378T>A[d] (Hmz)	p.Asp126Glu	C0	83±30	29±14	13±18
	c.8737G>T (Hmz)	p.Asp2913Tyr	C65			
53011A1	c.1156A>G	p.Arg386Gly	C45	100±0	67±14	38±11
	c.8461_8463delATG	p.Met2821del	Amino acid deletion			
56525A2	c.7985T>A (Hmz)	p.Val2662Asp	C65	96±25	44±12	17±22
60669A1	c.6491A>C	p.Glu2164Ala	C65	82±12	109±22	59±5
	c.6115G>A	p.Glu2039Lys[b]	C55			
63021A1	c.7985T>A (Hmz)	p.Val2662Asp	C65	80±1	27±16	23±10
63021A2	c.7985T>A (Hmz)	p.Val2662Asp	C65	107±21	32±15	23±18
WTs	WT	WT	NA	100±21	100±9	60±13
A-T	c.2483delA	p.Lys828SerfsX8	A-T control	29±3	Null	NA
	c.3511C>T	p.Gln1171X				

Abbreviations: A-T: ataxia telangiectasia; Hmz: homozygous mutation; LCL, lymphoblastoid cell line; NA: not applicable; ND: not done; WT, wild type.
Gray shading represents significant differences with WT.
[a]Expressed as the mean ± SD of three independent experiments.
[b]Amino-acid changes previously reported in A-T patients.
[c]rs56398245.
[d]rs2234997.

found in WT cell lines), moderately decrease in 12 cases (20 to 61% of normal *ATM* level) and normal in 2 cases (38437A1 and 60669A1; see Table 2). As expected, the LCL derived from the non-A-T patient 38437A1 presented normal *ATM* expression. Cell lines from different individuals or families carrying the same missense mutation presented similar levels of *ATM* expression. In comparison, *MRE11*, aprataxin and senataxin analyzed for differential diagnosis by western blotting were found normal (data not shown).

These expression defects could be due to transcriptional deregulation, which was tested by quantitative RT-PCR in mutant cell lines (Table 2). *ATM* transcripts were markedly decreased (29% of WT level) in the A-T control cell line carrying nonsense mutations, as a possible consequence of nonsense-mediated mRNA decay.[26] Accordingly, patient cell lines carrying an allele with nonsense mutations or splice defects introducing a frameshift had a twofold decrease in *ATM* transcripts (range 46–53% of WT level). Cell lines carrying only missense mutations or a short in-frame deletion had *ATM* transcripts in a range from 60 to 108% of WT level. These results demonstrate that transcriptional deregulation does not explain the decrease in *ATM* protein observed in LCLs bearing missense mutations.

ATM localization

ATM defects could also be related to its abnormal location.[22] Normal nuclear fraction was found to represent more than half of total *ATM* (60 ± 13%) in four WT cell lines (Figure 3a and Supplementary Figure 2). This fraction was measured in the series of patient cell lines and found significantly decreased (nuclear fraction representing 11–48% of total *ATM*) in 12 out of the 17 cell lines, all presenting a low expression of *ATM*. Consistently with western blot analysis, an abnormal cytoplasmic localization of *ATM* was evidenced by immunofluorescence for the 56525A2, 63021A2, 38563A1 and 53011A1 cell lines, which expressed sufficient ATM protein for detection (Figure 3b). No *ATM* could be detected in the A-T control cell line, demonstrating the specificity of the immunofluorescence (Figure 3b). Five of the cell lines presented no significantly abnormal localization of *ATM* (nuclear fraction: 39–59%), including the two cell lines with no decrease in *ATM* expression. These data suggested a link between *ATM* underexpression and abnormal cytoplasmic localization. Interestingly, the total *ATM* protein level was found to positively correlate with its nuclear localization (Pearson's test, $r=0.716$, $P<0.0006$; Figure 3c). This correlation was still significant in the subgroup with

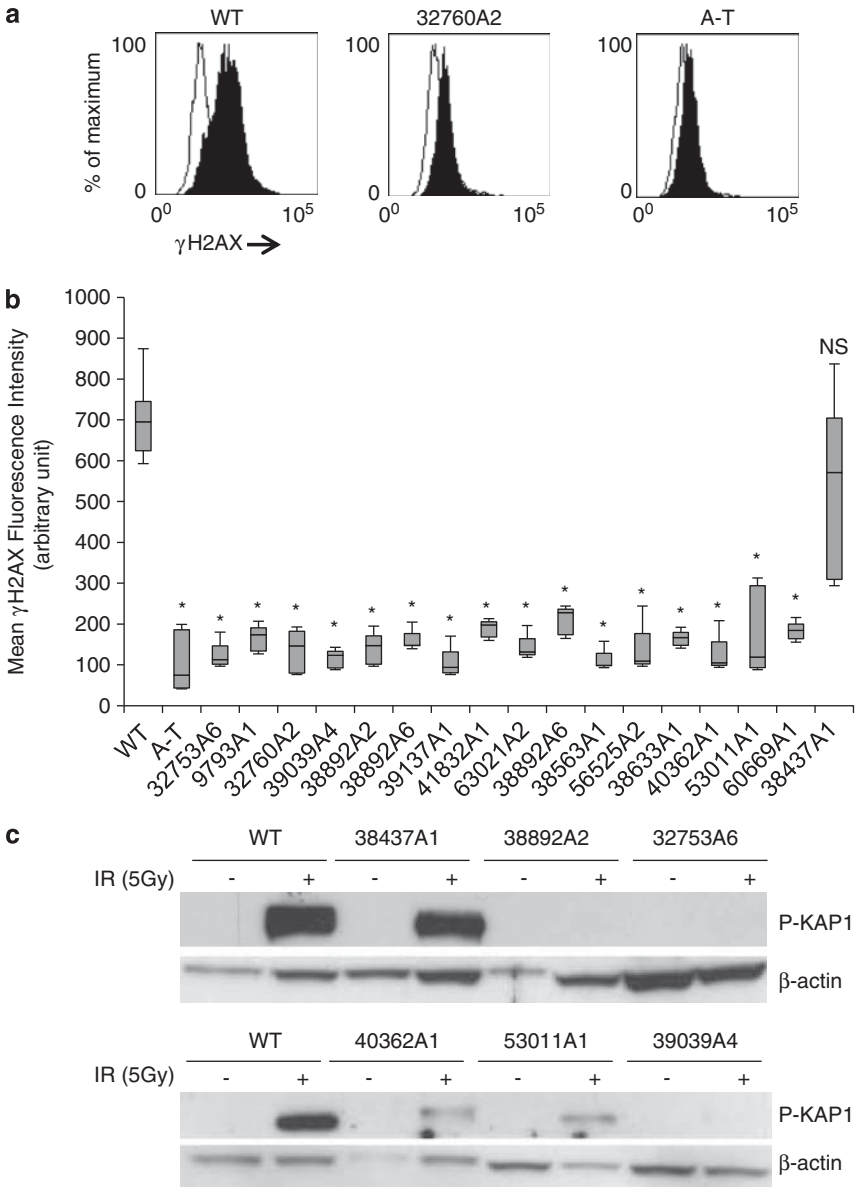

Figure 1 Response to IR. (**a**) *H2AX* phosphorylation in response to IR, 1.5 h after 5 Gy irradiation. *H2AX* fluorescence intensity was analyzed as an FL1-FITC histogram. Filled histogram: irradiated cells; empty histogram: untreated cells. (**b**) *H2AX* phosphorylation was measured by FACS and expressed as the difference with basal level (0 Gy). The box plot represents the mean and SD of at least three experiments. WT represents the mean and SD of nine normal cell lines. The significance of each sample *versus* WT is indicated above each column; NS, not significant; $*P<0.001$. (**c**) Analysis of *KAP1* phosphorylation 1 h after 5 Gy irradiation in cell lines derived from 17 patients bearing *ATM* missense mutations. *β*-actin is used as a loading control. WT cell line; A-T: A-T cell line carrying two truncating mutations in the *ATM* gene.

decreased *ATM* values (Pearson's test, $r=0.614$, $P<0.02$). This suggests that mutated *ATM* decreased protein level and mislocalization may be linked to a common mechanism. A noteworthy exception of this rule was the 386633A1 cell line, presenting decreased *ATM* expression and no abnormal protein localization.

DISCUSSION

Determining the clinical significance of missense variants is a recurrent problem in medical genetics. In this study, we characterized 17 LCLs bearing *ATM* missense mutations for *ATM* function, expression and localization. A total of 16 of these cases had a clinical diagnosis of A-T according to Micol *et al*,[14] as they presented (1) ataxia and at least two of the other five signs listed above: (2) oculocutaneous telangiectasia, (3) recurrent infections, (4) low serum IgA level, (5) high serum AFP and (6) specific karyotype abnormalities. For these 16 A-T cases, *ATM* function was consistently impaired and for 15 out of 16 cases either *ATM* expression level or cellular location or both were abnormal, strengthening the clinical diagnosis of A-T. The additional patient 38437A1 was included in this study because of some clinical features of A-T and the detection of two *ATM* missense mutations and a 6 bp intronic deletion without predicted splicing effects. However, these missense mutations had rather conservative amino-acid change (C0 A-GVGD score) and one was recently described as a SNP with a minor allelic frequency of 0.023 (rs56398245, http://www.ncbi.nlm.nih.gov/SNP/). Her clinical features were ataxia and elevated AFP (eightfold), but no telangiectasia at the age of 7 years old, no

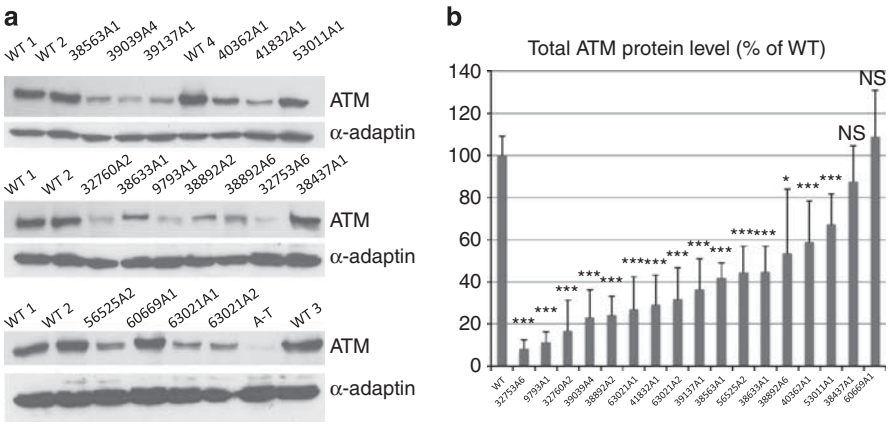

Figure 2 Western blot analysis of *ATM*. (**a**) Analysis of *ATM* protein level in cell lines derived from 17 patients bearing *ATM* missense mutations. α-Adaptin is used as a loading control. WT1-3 are WT cell lines, WT4 carries *ATM* SNP rs1800058 at the heterozygote state and an A-T cell line carries two truncating mutations in the *ATM* gene. This experiment is representative of at least three assays per sample. (**b**) Quantification was performed using ImageJ software. The histogram and error bars represent the mean and SD of *ATM* levels related to α-adaptin calculated from three independent western blots. The significance of each sample *versus* the control is indicated above each column; NS, not significant; $*P<0.05$ and $***P<0.001$.

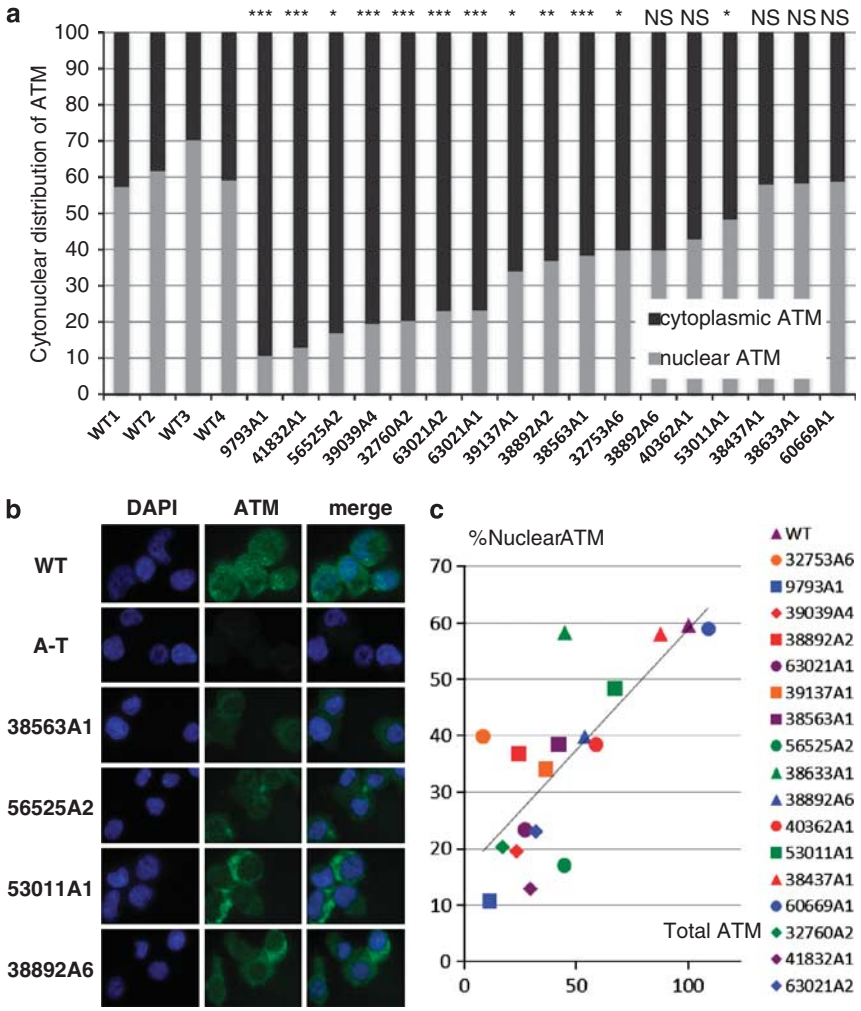

Figure 3 Analysis of *ATM* subcellular localization. (**a**) The histograms represent the mean fraction of nuclear (light gray) *versus* cytoplasmic (dark gray) *ATM* calculated from three independent experiments. WT1-3 are WT cell lines, WT4 carries *ATM* SNP rs1800058 at the heterozygote state. Samples showing a significantly lower nuclear fraction as compared with WT controls are indicated by; NS, not significant; $*P<0.05$, $**P<0.01$ and $***P<0.001$. (**b**) Localization of *ATM* by immunofluorescence. Representative images of four *ATM* missense mutation bearing cell lines are shown, together with WT and A-T cell lines as positive and negative controls. DNA is stained with DAPI (magnification ×1000). (**c**) Graph illustrating the correlation between *ATM* protein expression (expressed as percentage of normal *ATM* level on the *x*-axis) and nuclear fraction (expressed as percentage of total *ATM* level on the *y*-axis).

karyotype abnormality and no immune deficiency. Furthermore this patient presented facial dysmorphia and cerebral palsy that are rarely associated with A-T. The cell line derived from this patient displayed neither biochemical nor functional *ATM* defects, suggesting that these *ATM* missense mutations are not causative. Differential diagnosis includes AOA2, which is also associated with mild elevation of AFP, but no abnormality of *SETX* was detected and diagnosis is still pending.

In this study, biochemical and functional analyses supported the A-T diagnosis that was made on the basis of clinical features for 16 patients all presenting abnormal *ATM* expression, localization or *ATM* dysfunction and to exclude the A-T diagnosis for the patient with a pending diagnosis as she presented no *ATM* biochemical or functional abnormalities. Our series included 12 patients with missense mutations and without any detectable ATM kinase activity and accordingly, typical severe clinical features. The two remaining patients had milder or atypical A-T phenotypes. Case 40362A1 had a late onset ataxia (10 years) with neither telangiectasia nor clinical immunodeficiency, associated with a slight decrease in *ATM* expression, no *ATM* mislocalization and more importantly a residual P-*KAP1* response to IR, which may explain the milder disease. Case 9793A1 was a female patient with late onset ataxia, who survived until the age of 44 when she succumbed from acute adverse effects following breast cancer radiotherapy. Contrasting with the mild phenotype, this case was associated with a marked decrease in *ATM* protein (11% of the WT), a severe abnormal localization of *ATM* (with a nuclear fraction of 11%) and a response to IR, which was similar to an A-T control cell line. Two genetic mutations were found: one leading to an in-frame deletion of 29 amino acids and a missense mutation with a C0 score predicted to have low or null impact on protein function. However, whether these mutations were on different alleles could not be determined and one cannot exclude an undetected deep intronic mutation in this patient. Finally, case 53011A1 with early onset severe A-T presented residual P-*KAP1* response. Altogether in this small series of A-T cases, it was difficult to correlate the clinical evolution from our biochemical and functional *ATM* characterization, and role of modifier genes cannot be excluded. Future evaluation of newly identified functions of *ATM*,[8,9,27] may give important clues for mutation/phenotype relationship.

In agreement with previous studies,[19,28–32] we showed a decreased *ATM* protein in 14 of the 16 A-T confirmed cell lines. Recent studies based on transfection of *ATM* constructs carrying various missense mutations showed that some missense mutations were associated with decreased *ATM* protein expression.[17–19] The present study confirms that this phenomenon is also observed for endogenous *ATM* expression and is frequently associated with *ATM* missense mutations. Out of the two cases of our A-T series with normal *ATM* expression, one was bearing the c.6115G>A;p.Glu2039Lys mutation, which was modeled by Barone *et al*[18] and shown to lead to a stable *ATM* protein with little kinase activity.

Nuclear localization of *ATM* is crucial to allow correct DNA damage signaling.[22] A new finding of this study is the abnormal cytoplasmic localization of several mutated *ATM* products. The mechanisms underlying *ATM* localization have not yet been elucidated. Only one mutation in our series was located in the NLS of *ATM* (case 53011A1), and so impairment of the binding to importin could not be the general mechanism underlying our observation. Interestingly, our series include two changes of the same Asp2708 codon with different consequences: Asp2708Glu leading to a normal cytonuclear ratio, and Asp2708Asn – a nonpolar neutral *versus* acidic amino-acid change – to a cytoplasmic localization, suggesting that subtle conformation changes of the *ATM* protein may have marked consequences on its fate.

Out of the 14 A-T cell lines with underexpression, 13 presented a moderately to drastic abnormal cytoplasmic localization. Conversely, the two cases without *ATM* underexpression had normal protein localization. The link between abnormal cytoplasmic localization and decreased *ATM* expression is suggestive of exposure of cytoplasmic *ATM* to proteases and subsequent *ATM* degradation. Previous studies have reported that *ATM* can be a target for caspase 3 and caspase 7 under apoptotic conditions induced by irradiation or various agents,[33–35] but inhibition of caspase activity failed to restore *ATM* protein level as well as the treatment by the export-inhibiting drug leptomycin B (Jacquemin *et al*, 2010 unpublished data). Alternatively, as recently reported, amino-acid changes can affect *ATM* conformation, post-translational modification or protein–protein interaction sites involved in protein localization and stability,[18] but measured half life of mutated *ATM* proteins was not found decreased as compared with WT protein (Jacquemin *et al*, 2010 unpublished data). Furthermore case 32753A6 with major underexpression but normal localization and conservative amino-acid change indicates that each mutation could have peculiar consequences on *ATM* protein fate. However, understanding of the mechanisms underlying *ATM* underexpression and mislocalization could be critical to design new pharmacological strategies able to reverse these phenomena in A-T patients bearing missense mutations.

CONFLICT OF INTEREST

The authors declare no conflict of interest.

ACKNOWLEDGEMENTS

We thank Dr Debré, Dr Barbier, Pr Cosset, Pr Echenne, Dr Perelman, Dr Ponsot, Dr Pedespan, Dr Philip, Dr Leheup, Dr Jonyeaux, Dr Nguyen, Dr Delobel, Dr Guillot, Dr Soete, Dr Rivier and Dr Bordigoni for addressing patients, Genethon for access to cell lines, and the Institut Curie sequencing facility. VJ, SJ and GR are supported by grants from Association pour la Recherche sur le Cancer (ARC), from the Translational Department of Institut Curie, and the Ligue Nationale Contre le Cancer, respectively.

1 Boder E, Sedgwick RP: Ataxia-telangiectasia; a familial syndrome of progressive cerebellar ataxia, oculocutaneous telangiectasia and frequent pulmonary infection. *Pediatrics* 1958; **21**: 526–554.
2 Chun HH, Gatti RA: Ataxia-telangiectasia, an evolving phenotype. *DNA Repair (Amst)* 2004; **3**: 1187–1196.
3 Aurias A, Dutrillaux B, Buriot D, Lejeune J: High frequencies of inversions and translocations of chromosomes 7 and 14 in ataxia telangiectasia. *Mutat Res* 1980; **69**: 369–374.
4 Savitsky K, Bar-Shira A, Gilad S *et al*: A single ataxia telangiectasia gene with a product similar to PI-3 kinase. *Science* 1995; **268**: 1749–1753.
5 Lavin MF: Ataxia-telangiectasia: from a rare disorder to a paradigm for cell signalling and cancer. *Nat Rev Mol Cell Biol* 2008; **9**: 759–769.
6 Watters D, Kedar P, Spring K *et al*: Localization of a portion of extranuclear *ATM* to peroxisomes. *J Biol Chem* 1999; **274**: 34277–34282.
7 Li J, Han YR, Plummer MR, Herrup K: Cytoplasmic *ATM* in neurons modulates synaptic function. *Curr Biol* 2009; **19**: 2091–2096.
8 Alexander A, Cai SL, Kim J *et al*: *ATM* signals to TSC2 in the cytoplasm to regulate mTORC1 in response to ROS. *Proc Natl Acad Sci USA* 2010; **107**: 4153–4158.
9 Cam H, Easton JB, High A, Houghton PJ: mTORC1 signaling under hypoxic conditions is controlled by *ATM*-dependent phosphorylation of HIF-1alpha. *Mol Cell* 2010; **40**: 509–520.
10 Wright J, Teraoka S, Onengut S *et al*: A high frequency of distinct *ATM* gene mutations in ataxia-telangiectasia. *Am J Hum Genet* 1996; **59**: 839–846.
11 Concannon P, Gatti RA: Diversity of *ATM* gene mutations detected in patients with ataxia- telangiectasia. *Hum Mutat* 1997; **10**: 100–107.
12 Li A, Swift M: Mutations at the ataxia-telangiectasia locus and clinical phenotypes of A-T patients. *Am J Med Genet* 2000; **92**: 170–177.
13 Gilad S, Khosravi R, Shkedy D *et al*: Predominance of null mutations in ataxia-telangiectasia. *Hum Mol Genet* 1996; **5**: 433–439.

14 Micol R, Ben Slama L, Suarez F *et al*: Morbidity and mortality from ataxia-telangiectasia are associated with *ATM* genotype. *J Allergy Clin Immunol* 2011; **128**: 382–389.
15 Stewart GS, Last JI, Stankovic T *et al*: Residual ataxia telangiectasia mutated protein function in cells from ataxia telangiectasia patients, with 5762ins137 and 7271T→G mutations, showing a less severe phenotype. *J Biol Chem* 2001; **276**: 30133–30141.
16 Verhagen MM, Abdo WF, Willemsen MA *et al*: Clinical spectrum of ataxia-telangiectasia in adulthood. *Neurology* 2009; **73**: 430–437.
17 Mitui M, Nahas SA, Du LT *et al*: Functional and computational assessment of missense variants in the ataxia-telangiectasia mutated (*ATM*) gene: mutations with increased cancer risk. *Hum Mutat* 2009; **30**: 12–21.
18 Barone G, Groom A, Reiman A, Srinivasan V, Byrd PJ, Taylor AM: Modeling *ATM* mutant proteins from missense changes confirms retained kinase activity. *Hum Mutat* 2009; **30**: 1222–1230.
19 Scott SP, Bendix R, Chen P, Clark R, Dork T, Lavin MF: Missense mutations but not allelic variants alter the function of *ATM* by dominant interference in patients with breast cancer. *Proc Natl Acad Sci USA* 2002; **99**: 925–930.
20 Houdayer C, Dehainault C, Mattler C *et al*: Evaluation of in silico splice tools for decision-making in molecular diagnosis. *Hum Mutat* 2008; **29**: 975–982.
21 Olive PL: Detection of DNA damage in individual cells by analysis of histone *H2AX* phosphorylation. *Methods Cell Biol* 2004; **75**: 355–373.
22 Young DB, Jonnalagadda J, Gatei M, Jans DA, Meyn S, Khanna KK: Identification of domains of ataxia-telangiectasia mutated required for nuclear localization and chromatin association. *J Biol Chem* 2005; **280**: 27587–27594.
23 Tavtigian SV, Oefner PJ, Babikyan D *et al*: Rare, evolutionarily unlikely missense substitutions in *ATM* confer increased risk of breast cancer. *Am J Hum Genet* 2009; **85**: 427–446.
24 Porcedda P, Turinetto V, Brusco A *et al*: A rapid flow cytometry test based on histone *H2AX* phosphorylation for the sensitive and specific diagnosis of ataxia telangiectasia. *Cytometry A* 2008; **73**: 508–516.
25 Ziv Y, Bielopolski D, Galanty Y *et al*: Chromatin relaxation in response to DNA double-strand breaks is modulated by a novel *ATM*- and KAP-1 dependent pathway. *Nat Cell Biol* 2006; **8**: 870–876.
26 Isken O, Maquat LE: Quality control of eukaryotic mRNA: safeguarding cells from abnormal mRNA function. *Genes Dev* 2007; **21**: 1833–1856.
27 Guo Z, Kozlov S, Lavin MF, Person MD, Paull TT: *ATM* activation by oxidative stress. *Science* 2010; **330**: 517–521.
28 Stankovic T, Kidd AM, Sutcliffe A *et al*: *ATM* mutations and phenotypes in ataxia-telangiectasia families in the British Isles: expression of mutant *ATM* and the risk of leukemia, lymphoma, and breast cancer. *Am J Hum Genet* 1998; **62**: 334–345.
29 Sandoval N, Platzer M, Rosenthal A *et al*: Characterization of *ATM* gene mutations in 66 ataxia telangiectasia families. *Hum Mol Genet* 1999; **8**: 69–79.
30 Becker-Catania SG, Chen G, Hwang MJ *et al*: Ataxia-telangiectasia: phenotype/genotype studies of *ATM* protein expression, mutations, and radiosensitivity. *Mol Genet Metab* 2000; **70**: 122–133.
31 Lakin ND, Weber P, Stankovic T, Rottinghaus ST, Taylor AM, Jackson SP: Analysis of the *ATM* protein in wild-type and ataxia telangiectasia cells. *Oncogene* 1996; **13**: 2707–2716.
32 Angele S, Lauge A, Fernet M *et al*: Phenotypic cellular characterization of an ataxia telangiectasia patient carrying a causal homozygous missense mutation. *Hum Mutat* 2003; **21**: 169–170.
33 Smith GC, d'Adda di Fagagna F, Lakin ND, Jackson SP: Cleavage and inactivation of *ATM* during apoptosis. *Mol Cell Biol* 1999; **19**: 6076–6084.
34 Tong X, Liu B, Dong Y, Sun Z: Cleavage of *ATM* during radiation-induced apoptosis: caspase-3-like apoptotic protease as a candidate. *Int J Radiat Biol* 2000; **76**: 1387–1395.
35 Hotti A, Jarvinen K, Siivola P, Holtta E: Caspases and mitochondria in c-Myc-induced apoptosis: identification of *ATM* as a new target of caspases. *Oncogene* 2000; **19**: 2354–2362.

Supplementary Information accompanies the paper on European Journal of Human Genetics website (http://www.nature.com/ejhg)